Title	Observation of Keyhole and Molten Pool Behaviour in High Power Laser Welding : Mechanism of Porosity Formation and Its Suppression Method
Author(s)	Matsunawa, Akira; Seto, Naoki; Kim, Jong-Do et al.
Citation	Transactions of JWRI. 2001, 30(1), p. 13-27
Version Type	VoR
URL	https://doi.org/10.18910/11785
rights	
Note	

Observation of Keyhole and Molten Pool Behaviour

in High Power Laser Welding†

- Mechanism of Porosity Formation and Its Suppression Method -

Akira Matsunawa*, Naoki Seto**, Jong-Do Kim***, Masami Mizutani****
and Seiji Katayama*****

Abstract

In high power pulsed and CW laser welding, characteristic porosity is frequently formed in the weld metal, but its formation mechanism has not been well understood. Therefore, the authors have conducted systematic studies of porosity formation in relation to keyhole dyanamics[1-4]. They have revealed that many bubbles are formed mainly from the bottom tip of a keyhole by intense evaporation of metal. It has been also revealed that the keyhole frequently fluctuates and changes its size and shape corresponding to the intermittent bubble formation. The majority of bubbles are trapped at the solidifying front in the rear part of the molten pool. However, there are few reports that deal the simultaneous observation of keyhole and plasma dynamic behaviour as well as the formation of bubbles and porosity. In this study, therefore, the interrelationship between keyhole and plasma behaviour was examined by the optical and X-ray transmission observation methods. The systematic observations of keyhole, molten pool and laser induced plasma have revealed that the keyhole instability is enhanced by the localized intense evaporation of metal on the front keyhole wall and this unstable behaviour leads to the formation of characteristic porosity. It has been also revealed that the porosity can be suppressed successfully by the use of pulse modulation laser and pure nitrogen shield.

KEY WORDS: (Laser welding), (Keyhole), (Keyhole instability), (Liquid motion), (High speed photography), (X-ray transmission method), (Porosity), (Suppression of porosity)

1. Introduction

Generation of solidification cracking and porosity are two major serious imperfections in laser welding. The authors have conducted experimental and theoretical studies on their mechanisms and suppression methods[1-4]. The thermal cycle in laser welding is extremely high by the nature of concentrated heat source, and thus the susceptibility of solidification cracking increases as compared with arc welding. On this matter, the authors[5] have revealed a mechanism through theoretical work on rapid solidification process and have shown that the addition of controlled heat during solidification can regulate the growth rate of dendrites, which effectively reduces the hot cracking susceptibility.

Cavity or porosity formation is another important problem to be solved in high power laser welding. Hydrogen is generally one of the major causes of porosity formation in fusion welding, particularly in Aluminium alloys. Hydrogen causes many small blow holes in Al-alloys in laser welding, too. In particular, the average temperature of the laser weld pool is quite high, and hence the solubility of Hydrogen in the pool is increased more than in arc welding. Therefore, hydrogen induced porosity is enhanced in laser welding. However, the very characteristic porosity is formed in keyhole laser welding, which is reflected by the large cavities in the

middle and lower part of weld metal[1-4]. The author has revealed, by the direct observation of keyhole using the high speed X-ray photographic method, that the absorption of the laser beam does not occur uniformly on the keyhole front wall, but changes temporally and spatially, and thus the evaporation site on the front wall changes its position with time[2-4]. Due to the strong dynamic pressure of the evaporated metal vapour jet, the rear wall of the keyhole fluctuates violently, and metal jet ejected from the keyhole opening changes its direction and speed temporally. The unstable keyhole phenomena enhance the entrapment of shielding gas into the keyhole and result in the formation of characteristic porosity.

This paper will systematically describe the observed keyhole and weld pool dynamics, mechanisms and suppression methods of the porosity generation in pulsed and CW laser welding.
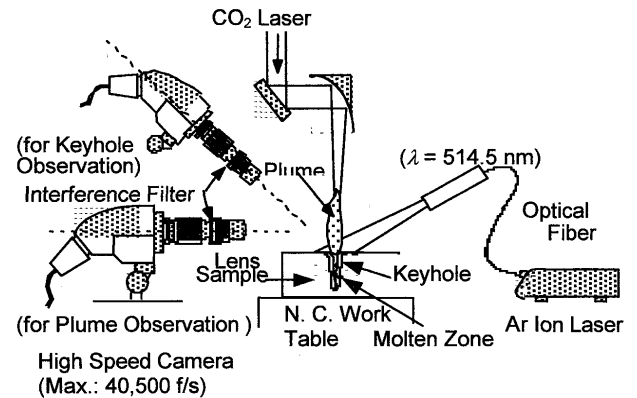
2. Observation Methods of Keyhole Dynamics

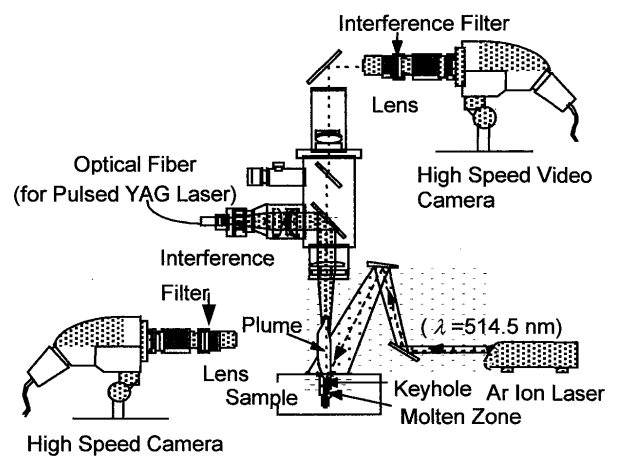### 2.1 Observation of keyhole and weld pool by optical method

Figure 1 shows the simultaneous observation method of keyhole and weld pool behaviour during the YAG and CO_2 laser welding. The molten pool is illuminated by an Argon ion laser (Wavelength: 514.5 nm) and the image of the keyhole can be taken by high speed video camera (Max. 40,500 f/s) using an interference filter that transmits the wavelength of the Argon ion laser. The laser-induced plume is simultaneously photographed by another high speed video or streak camera through a band pass filter which cuts the wavelength of the Argon ion laser.

2.2 Observation of keyhole dynamics in metal by X-ray transmission imaging system

Keyhole behaviour in the metal can not be observed by optical methods. The author's have, therefore, developed a high speed X-ray transmission imaging

(a) Pulsed YAG laser welding

(b) CW CO_2 laser welding

Fig. 1 Simultaneous observation of keyhole and laser induced plume by optical method

system shown in Fig. 2. The idea is not new one but was used by Arata and others[7] to observe keyhole dynamics of EB welding in the 1980's. However, the spatial resolution of the X-ray image was not sufficient to detect the shallow keyhole of laser welding. The recent X-ray source is micro-focused and the fluorescent image intensifier that converts the X-ray image to a visible one has been improved in sensitivity. The system shown in Fig. 2 employs a micro-focused X-ray source (Acceleration voltage: 170 kV; Min. diameter of X-ray: 10 μm, usually 100 μm) and also uses a visible-visible image intensifier. Therefore, the small keyhole of the laser weld pool can be magnified enough on the fluorescent converter to observe its behaviour. This system can take a high speed video image up to 5,000
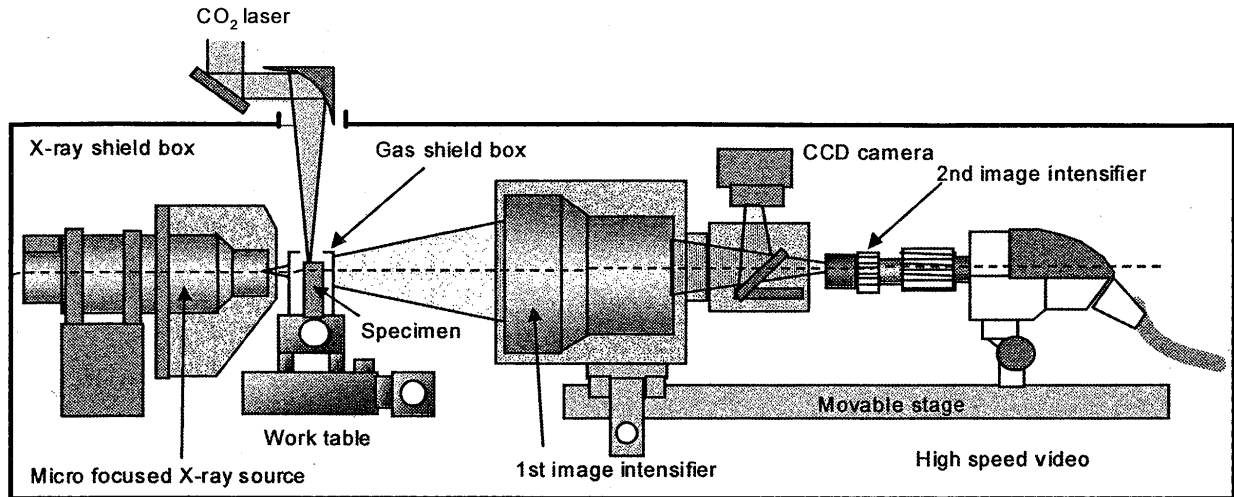
Fig. 2   X-ray transmission imaging system for observation of keyhole and weld pool dynamics
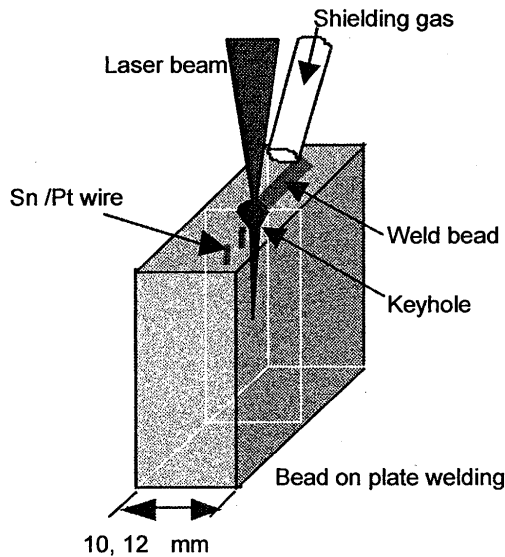
Fig. 3   Observation method of weld pool configuration

Fig. 4   Observation method of liquid motion in weld pool

flames per second (f/s).   In order to observe the weld pool configuration, a fine wire was buried along the weld line as shown in **Fig. 3**.   A Tin wire was used for Aluminum alloys and Platinum wire employed for steels because these materials have similar melting points and different X-ray absorption coefficients to base metals.

The liquid flow in the weld pool was observed by pre-placing fine Tungsten particles of 100 - 400 µm in diameter between the two thin plates as shown in **Fig. 4** and the traces of W-particles in the video images were analyzed.
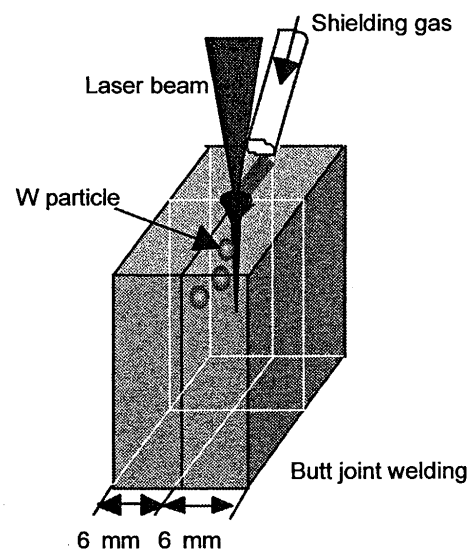
3.   Observed Results of Keyhole and Weld Pool Dynamics and Porosity Formation Mechanism

3.1 Pulsed YAG laser spot welding phenomena observed by optical and X-ray methods

Figure 5 shows an example of molten pool behaviour during and after pulsed YAG laser spot welding of A5083 alloy.   The pulse duration was 10 ms and its shape was almost rectangular.   The surface began to melt within 0.2 ms after laser initiation and melting developed by heat conduction at the beginning. However, about 1 ms after laser irradiation the pool surface was depressed at the central part by the intense evaporation of metal and a keyhole was clearly observed.

A5083; E_0 = 40 J/P, τ_p = 10 ms, f_d = 0 mm

(a) 0.18 ms   (b) 2.07 ms   (c) Keyhole 5.85 ms

(d) 6.73 ms   (e) 6.96 ms   (f) 9.96 ms

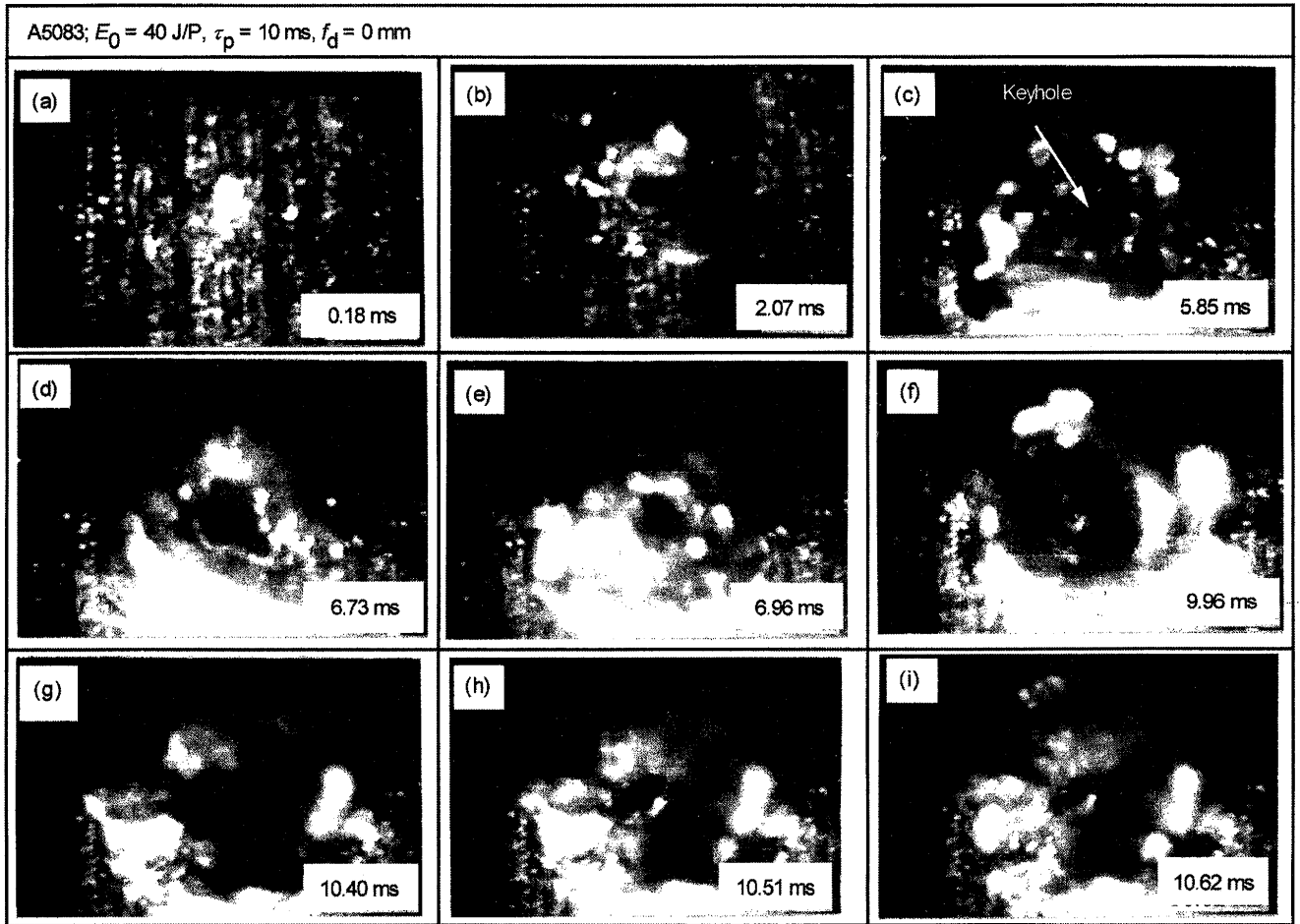(g) 10.40 ms   (h) 10.51 ms   (i) 10.62 ms

Fig. 5   Dynamic behaviours of keyhole opening in pulsed YAG laser spot welding with rectangular pulse shape
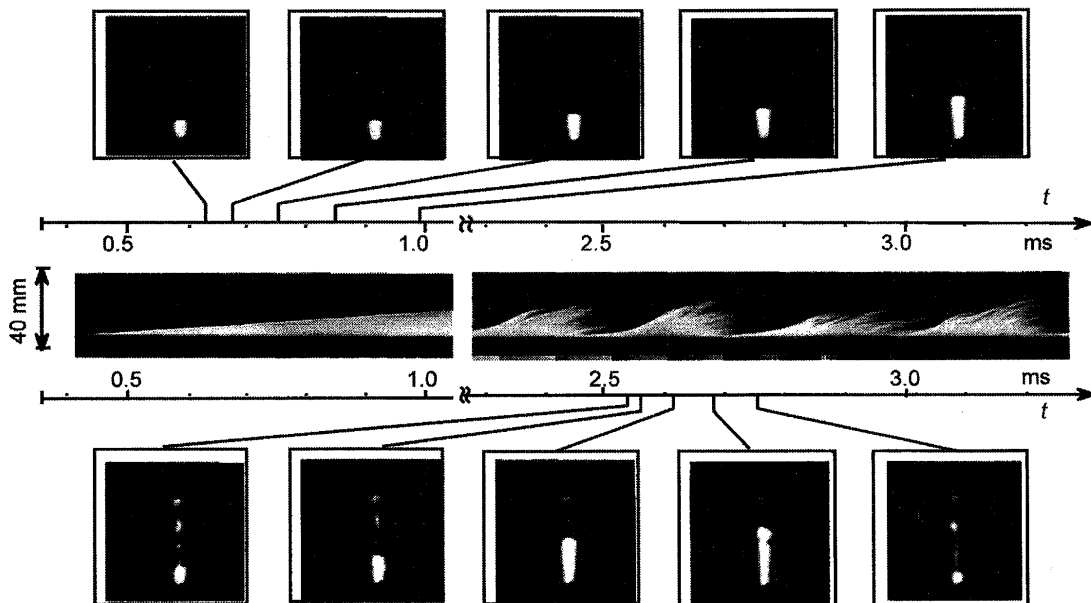
Fig. 6   Streak and flaming images of laser induced plume of Ti in pulsed YAG spot welding

(V_s = 86.12 m/s, R_t =1.16 ms, n_f = 40,500 f/s, τ_p = 7 ms, E_0 = 17.3 J/p)

As seen in the figure, the size and shape of keyhole opening fluctuated considerably in spite of the constant peak power of the pulse laser.   The beam diameter used was 700 μm, but the keyhole diameter changed its size from 100 to 700 μm and its fluctuation period was 350 to 500 μs.   After the laser termination, the keyhole opening

quickly closed within 0.8 ms though it took about 8 ms until the whole weld pool solidified. It was obvious from this observation that a keyhole was not stable but fluctuated violently even under the constant laser power. Such unstable keyhole behaviour was also seen in other materials but the fluctuation period was different depending on the material.

The dynamic behaviour of the plume was also simultaneously observed by high speed streak and video cameras. **Figure 6** shows the streak and flaming images of the laser induced plume. As seen in the pictures, the plume developed upward gradually at the beginning where a conduction mode welding was progressing However, once a keyhole was formed in the molten pool, the plume velocity fluctuated periodically and the plume velocity was extremely high at the beginning of each fluctuation. This periodic generation and extinction of laser plume coincided completely with the keyhole fluctuation shown in the previous Fig. 5. The result suggested that the beam energy was not uniformly absorbed on the keyhole wall but the evaporation site changed its position cyclically, and hence the keyhole as well as the molten pool was disturbed by the strong metallic vapour jet.

In the keyhole laser spot welding with a rectangular pulse shape, a large porosity or cavity was usually formed at the bottom of keyhole as seen in **Fig. 7**. This type of porosity is always formed in any metal, but more especially in the spot welding of Al alloys containing volatile elements such as Mg and Zn. The gas analysis of the pore showed that shielding gas and small amounts of air were detected[1]. It was also confirmed that Mg or Zn was enriched on the wall surface of cavity and their oxides were also detected if the shielding was not perfect. Therefore, metallic vapour is the major gas component inside the keyhole, and small amount of shielding gas and sometimes air were entrained into the keyhole during its fluctuation. As shown in the **Fig. 8** as well as previous Fig. 5, the top part of keyhole choked quickly after laser

termination and the shielding gas as well as metallic vapour were trapped, which led to the formation of large cavity.
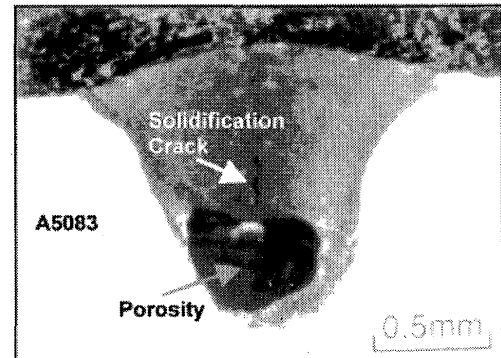

Fig. 7 Porosity formation in pulsed YAG laser spot welding with rectangular pulse (Aluminium alloy A5083; Pulse duration: 7 ms; Pulse energy: 31.7 J/p)
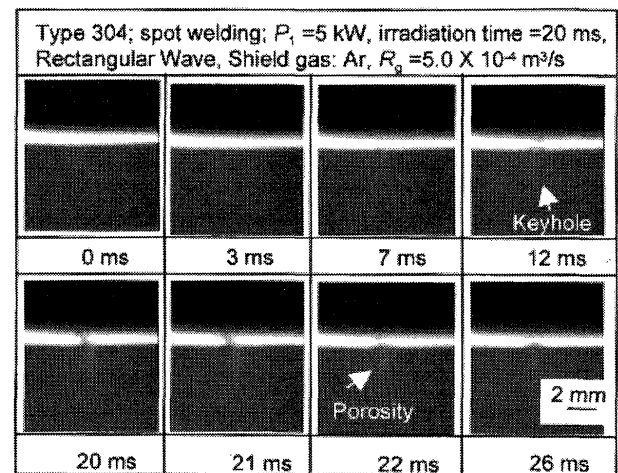

Fig. 8 Keyhole formation and collapse during and after laser irradiation of rectangular pulse

3.2 CW CO_2 welding phenomena observed by optical methods

Figure 9 represents the keyhole behaviour observed in CO_2 laser welding of 304 stainless steel in Ar shielding. In this picture a white round shape close to the molten pool front was the keyhole opening. The keyhole opening in pulsed laser spot welding was dark as shown in the Fig. 3. This is because the intensity of the Argon ion laser was not high enough to cancel the bright laser plasma in order to illuminate the whole weld pool. Fluctuation of the keyhole was much less than in spot welding but still the shape and size of the keyhole opening changed with time. It was also seen that bright

slag spots moved from the both side of keyhole to the rear part of the molten pool, and they turned their direction to forward along the center of weld pool. The speed of slag at the side of keyhole was about 1 m/s. Thus, a very quick circulation of liquid was observed on the molten pool surface.

It was also confirmed that the laser induced plume/plasma changed its evolution direction synchronized with the keyhole motion. Thus, the plume developed straight upward when the keyhole opening was large, while it tilted behind when keyhole size became small. If carefully observed, the rear part of molten pool, the large liquid wave propagated to rear side when keyhole was wide, and the reflected wave from the rear fusion boundary caused a narrowing of the keyhole

opening. When the fluctuation was large, porosity was always present, particularly in the welding of Al-Mg or Al-Zn alloys. As stated above, the keyhole is not quasi-stationary but fluctuates, even in continuous welding, and this instability is closely related to the large cavity formation.

Figure 10 shows the laser plasma in CW CO_2 laser welding of Al-alloy in Ar shield. There were 2 kinds of plasma found, i.e., the fluctuating metallic plasma ejected from the keyhole and the stationary Ar plasma along the beam axis. The inclination angle of the metallic plasma becomes less at higher welding speed, and there is no actual fluctuation at welding speeds higher than 100 mm/s. This indicates that a quasi-stationary state is achieved in very high speed welding.
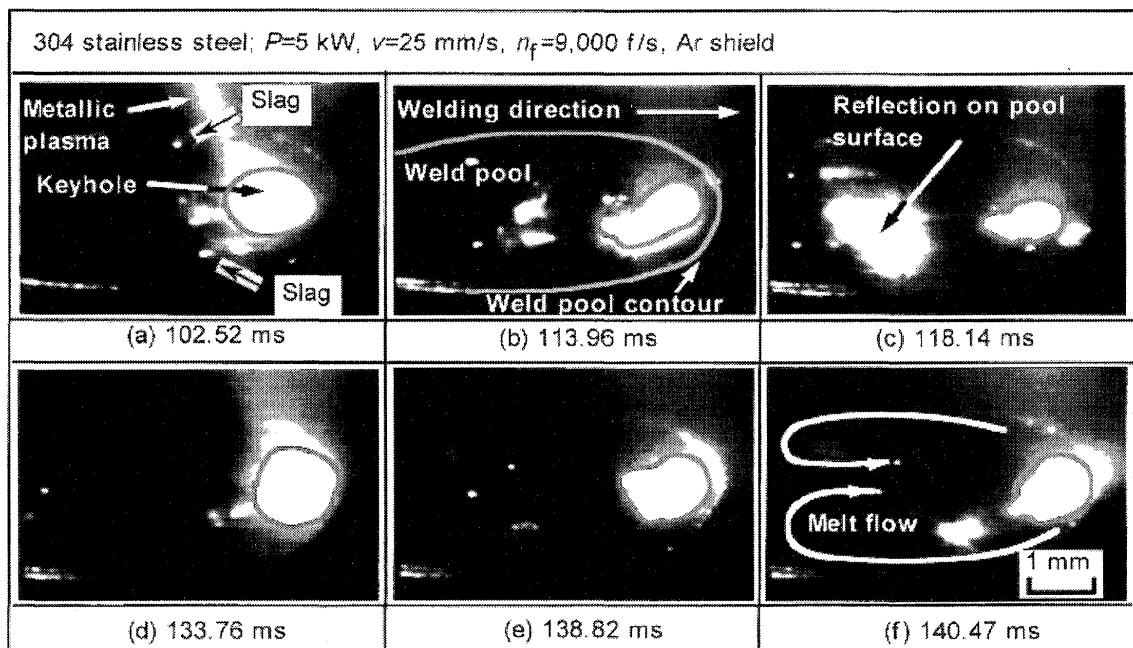

Fig. 9   Dynamic behaviours of keyhole opening and molten pool in CW CO_2 laser welding
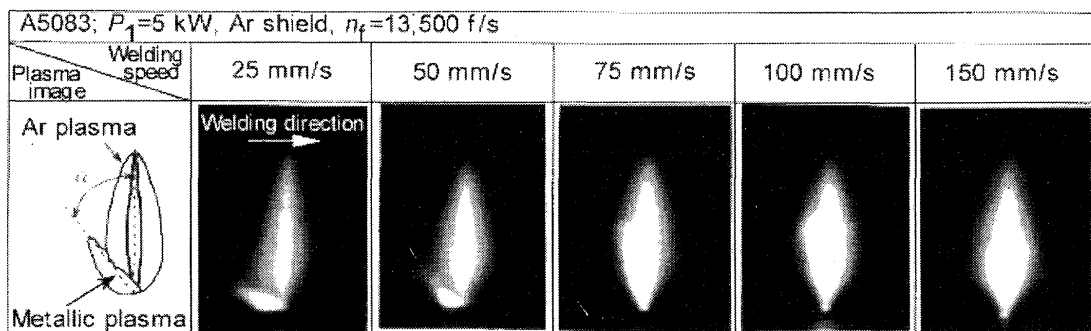

Fig. 10   Formation and behaviour of metallic and Argon plasmas in CW CO_2 laser welding

3.2 Observed keyhole and weld pool dynamics by X-ray methods in CW CO_2 laser welding

The above stated optical observations revealed that the keyhole was not stable but fluctuated considerably and this instability was closely related to the porosity formation. However, the actual porosity formation process in the molten pool was impossible to see by optical methods. The authors conducted direct observation of the keyhole in the metal by the X-ray method shown in the previous Fig. 2.

Figure 11 shows examples of X-ray transmission images taken by a high speed video camera during CO_2 laser welding of A5083 alloy in He shield and their schematic representation. It was clearly observed that the depth and shape of the keyhole fluctuated violently, and large bubbles were intermittently formed, mainly at the bottom of the keyhole, which were trapped by the solidifying wall during floating up and remained as porosity. On the rear wall of the keyhole, a deep depression of the wall was observed and it moved down
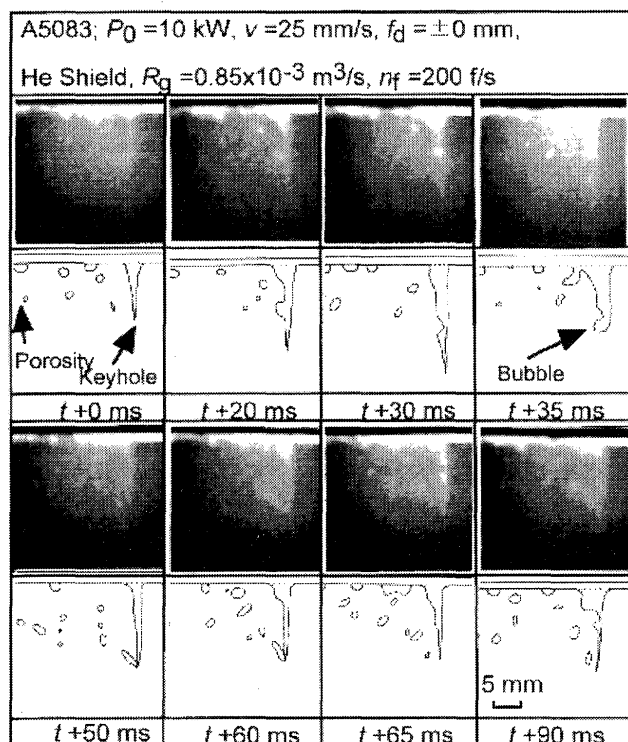
from the top to the bottom. On the keyhole front wall, opposite to the deep depression, the inclination angle of the wall was slightly changed. Namely, there was a small discontinuity in angle, or small hump on the front wall, which was also observed in electron beam welding by Arata and others in 1970s[7]. This meant that the evaporation of metal did not take place uniformly but locally on the keyhole front wall. As illustrated schematically in **Fig. 12**, the present authors estimate that the intense evaporation takes place at the hump due to the large angle to the incident beam, and the dynamic pressure of metallic vapour jet dents the rear wall of the keyhole. The same phenomena were observed in other materials such as stainless steels, ordinary steels, etc., in Ar and He shield.
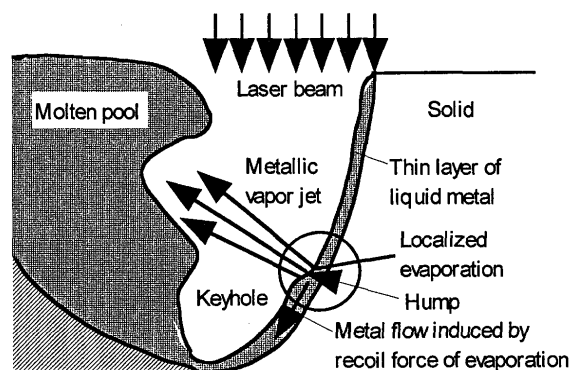

Fig. 12   Fluctuation of molten pool by localized intense evaporation of metal at keyhole front wall

As stated above, a keyhole is not in a stationary state but fluctuates dynamically in spite of the constant power CW laser welding. It used to be thought that a keyhole was in a quasi-stationary state under the pressure balance between the recoil pressure of evaporation and surface tension pressure (Laplacian pressure) as well as the hydrostatic pressure. It was also believed that the evaporation of metal took place uniformly on the keyhole wall. In fact, most of the existing models of keyhole welding[8-17] were constructed under the assumption of a quasi-stationary state. There were several reports which dealt with the oscillation of the keyhole[16, 17]. In these reports, too, the oscillation of the keyhole was treated as a small perturbation from the equilibrium condition.

Fig. 11   Dynamic behaviour of keyhole observed by X-ray method in CW CO_2 welding of Al-alloy

However, it is obvious from the above direct observations of keyhole dynamics that a static pressure balance is not held in laser welding and a more dynamic model is required. V. V. Semak, J. A. Hopkins, M. H. McCay and T. D. McCay[18, 19], R. Fabbro and A. Poueyo-Verwaerde[20], and A. Matsunawa and V. Semak[21, 22] assumed that the keyhole welding phenomenon was equivalent to that of laser drilling, and proposed dynamic models.
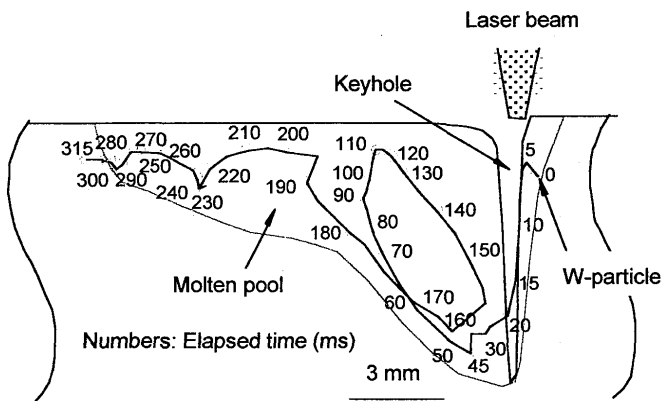

Fig. 13 Liquid flow observed by X-ray method (A5083; Butt welding; P_0 =10 kW, v = 25 mm/s, fd =±0 mm (f=381 mm), Assist gas: He, Rg = 8.5×10^{-4} m^3/s)

The metal flow in the molten pool was also observed by tracing the motion of small tungsten particles of 0.1 - 0.4 mm in diameter which were preplaced between two thin sheets. **Figure 13** illustrates an example of the trajectory of a W-particle in which the numbers show the elapsed time in milli-second since the W-particle began to move. As seen in the figure, a W-particle is moved down quickly along the front keyhole wall, at the speed of 0.4 m/s, to the bottom of keyhole by the strong downward stream, and then it moves along a strong eddy in the rear part of weld pool. The speed of the particle near the eddy reaches to 0.25 - 0.35 m/s, which is considerably fast compared with natural convection. The motion of a metallic vapour bubble shown in the previous Fig. 11 is very similar to the movement of W-particles. Namely, many of the large bubbles can not float up by buoyancy force but are entrained by the strong liquid metal flow and trapped at

the solidifying wall which results in the formation of large cavities.

Gas analysis was performed by a special method to drill the part of porosity in a high vacuum chamber and released gases were analyzed by Q-mass spectrometer as shown in **Fig. 14**. Analyzed results are tabulated in **Table 1**. The major gas was He shielding gas and the content of H_2 was not high. Small amounts of N_2 and Ar were also detected, which might be entrained air. **Figure 15** shows the SEM photos of fractured porosity surfaces on which the Mg/Al oxides and Mg-enriched fine particles are detected. Namely, the large cavities shown in Fig. 9

(a)   Location of porosity

(b)   Method of gas analysis in porosity in high vacuum
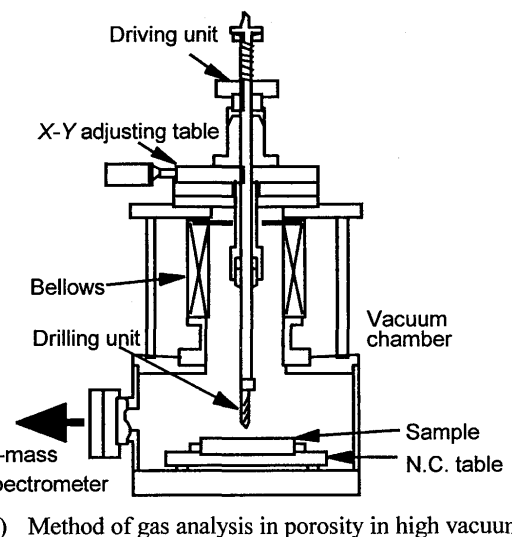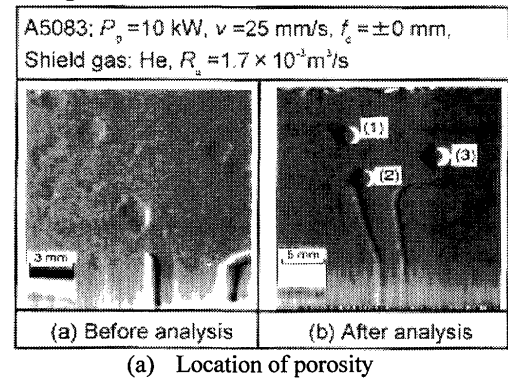
Fig. 14   Method of gas analysis of porosity in high vacuum

Table 1   Gas composition in porosity

Location	Composition (Vol. %)			
	H_2	He	N_2*	Ar*
(1)	3.31	95.9	0.21	0.55
(2)	12.6	86.8	–	0.58
(3)	8.13	90.7	0.47	0.68

*N_2 and Ar gases were supposed to be the entrained air.

A5083 (6 mmt); P_2 = 5 kW, v = 25 mm/s, f_z = 0 mm
Shielding gas: He, R =5.1 × 10⁻² m³/s

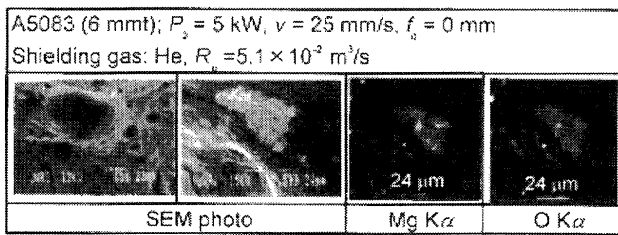| SEM photo | Mg Kα | O Kα |

Fig. 15   SEM photos of fractured surface of porosity

were primarily formed by metal vapour together with the entrapped shielding gas as well as air.

4. Suppression Methods for Porosity in Laser Welding

4.1 Suppression of porosity by wave form control in pulsed laser spot welding

As described in **3.1**, a large cavity is formed at the bottom of the keyhole when the laser power is shut down quickly. Figures **5** and **8** showed that the keyhole opening quickly closed after laser power termination, which caused the sudden collapse of the keyhole opening and the metal vapour and shielding gas are trapped in the keyhole. Therefore, it is necessary to stabilize the keyhole during cooling in order to prevent this collapse. The authors have developed a special pulsed YAG laser machine that is able to control the wave form in arbitrary shape.

Figure 16 shows the effect of a tailing wave after the sudden termination of the pulse in laser spot welding of 304 steel, showing that the gradual decay of power during cooling brings the position of porosity upward and finally porosity disappears completely. Thus, the keyhole must be gradually decreased in depth after the main pulse energy by providing the proper decaying power.

4.2 Suppression of porosity caused by metal vapour jet in the keyhole

Evaporation of metal in laser welding has an advantage in one sense forming deep penetration by the

(a) E_0=38.7 J/p
(b) E_0=43.0 J/p
(c) E_0=50.3 J/p
(d) E_0=57.2 J/p

Type 316; f = 150 mm, f_d=5 mm

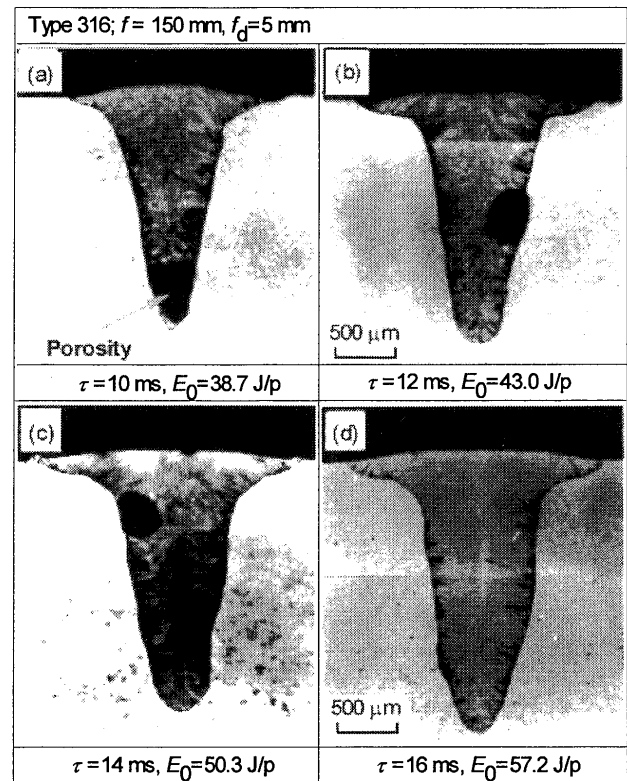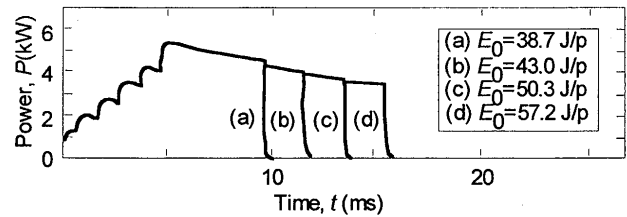| Porosity | 500 μm |
| τ = 10 ms, E_0=38.7 J/p | τ = 12 ms, E_0=43.0 J/p |
| τ =14 ms, E_0=50.3 J/p | τ =16 ms, E_0=57.2 J/p |

Fig. 16   Effect of tailing pulse on suppression of porosity in pulsed YAG laser spot welding

strong recoil pressure of vaporization. However, it is also a disadvantage that the strong vapour jet that is generated in the very deep keyhole welding (or welding of materials including volatile elements) induces the instability of the keyhole as well as the weld pool, and large porosity is easily formed. The essential means of reducing or suppressing this type of porosity is to keep the keyhole stable under the condition of quasi-stationary state but it is only possible to achieve this in very high speed welding[21].

Arata and others [7] showed in EB welding that use of two beams (Tandem Electron Beam Welding) or the oscillation of a single beam had an effect on suppression of porosity induced by vaporization of volatile elements.

The idea is also expected to be effective in laser welding.

It was already stated in Fig. 16 that the pulse shaping was very effective to avoid large porosity in pulsed spot welding. In continuous welding, too, proper pulse modulation was effective in reducing the porosity. **Figure 17** shows the effect of pulse modulation on the porosity formation. In CW laser welding a large number of pores induced by instability of keyhole are shown along the bead. However, the pulse modulation with proper duty cycle and frequency reduced the number of pores drastically. The reduction of pores was attributed to the fact that the holes formed in the previous pulse were effectively removed from the keyhole formed by the next pulse if the overlapping ratio was adequate. Optimum pulse modulation was also effective in achieving more stable keyhole motion by the forced oscillation, as Otto and others[24] mentioned. It will be absolutely necessary to employ pulse modulation techniques to avoid porosity formation in very high power deep penetration laser welding.

In CW laser welding, the angle of beam incidence has also a good effect on reduction of porosity formation.
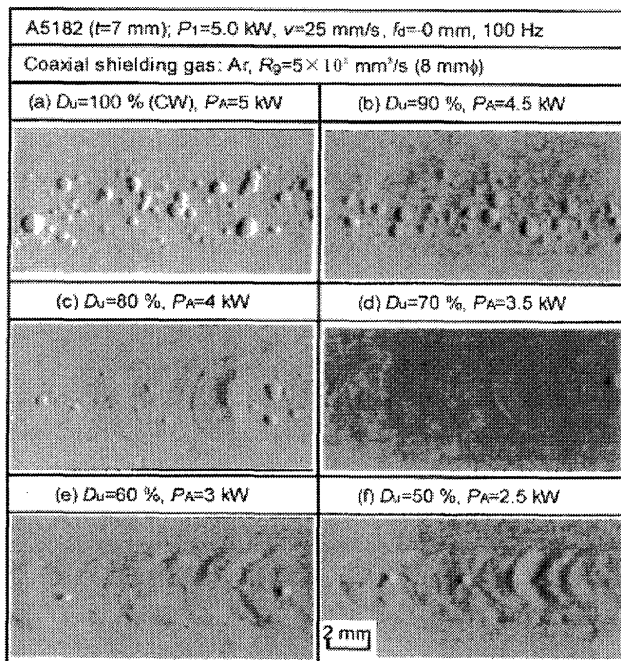
In case of a trailing angle of beam incidence, the porosity formation was greatly enhanced. While, in case of leading angle, the bubbles of metallic vapour and shielding gas were smoothly removed from the upper part of keyhole and porosity was effectively reduced.

4.3 Effect of shielding gas on suppression of porosity

Figure 18 shows the X-ray photos of laser weld metals of Aluminium alloy, type 304 stainless steel and low Carbon steel in a Helium and Nitrogen shield. In a He shield a great amount of porosity is shown in every metal, while no porosity is seen in Aluminium alloy and stainless steel with the N_2 shielding. In mild steel, on the other hand, small porosity is seen but its amount is greatly reduced compared with the He shield. The effect of N_2 on reduction of porosity is obvious.
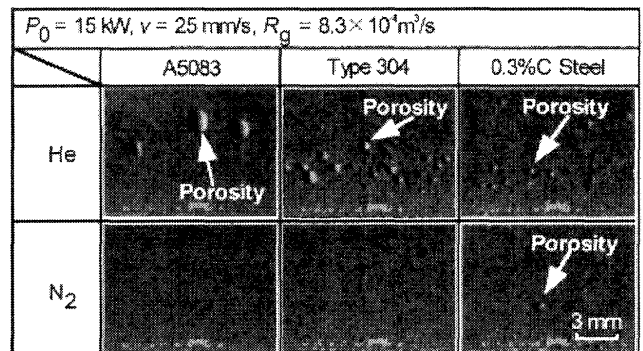
Fig. 18   Effect of shielding gas on reduction of porosity

It has been empirically known that the use of pure Nitrogen is very effective to avoid porosity in the CO_2 and YAG laser welding of austenitic stainless steel. On the contrary, CO_2 laser welding of Aluminium alloys in Nitrogen shielding brings no porosity formation, but not in YAG laser welding. In the case of austenitic stainless steel, it has been understood that the Nitrogen is soluble largely in the weld metal which leads to a reduction of the porosity formation. In fact, the amount of solute Nitrogen in weld metal is greatly increased, of the order of 1,000 ppm, particularly in CO_2 laser welding as shown in **Fig. 19**. The solute Nitrogen in the case of

Fig. 17   Effect of pulse modulation on reduction of porosity

Fig. 19   Increase in solute Nitrogen in weld metal
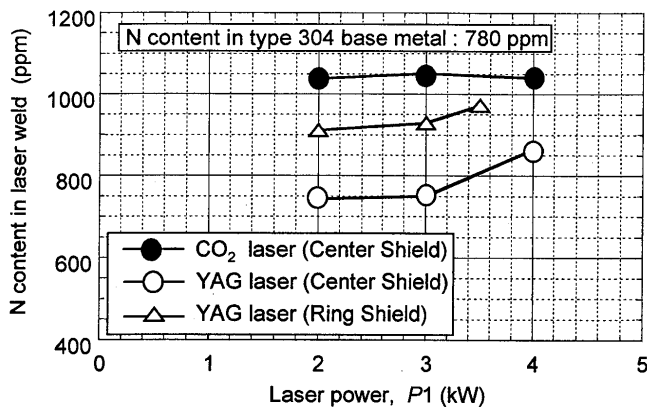in laser welding

Fig. 20   Effect of shielding gas on bead formation and micro-
structure of weld metal

YAG laser welding is lower than that in CO_2 laser welding, but still much higher than that in the base metal.

As to porosity suppression in Aluminium alloys in laser welding with a Nitrogen shield, the effect is only seen in CO_2 laser welding but not in YAG laser welding. As seen in **Fig. 20**, a large amount of AlN (Aluminium-Nitride) is presented in the CO_2 laser weld metal when the pure Nitrogen shield gas is used. As AlN has a higher melting point than that of Aluminium, the surface of the molten pool is covered by an AlN solid film, and hence severe undercutting is likely to appear in Nitrogen shielding. Due to this chemical reaction the porosity formation is effectively suppressed in CO_2 laser welding of Aluminium alloys in pure Nitrogen shield. While, in YAG laser welding in Nitrogen shielding, no AlN is formed and porosity can not be suppressed. The fact suggests that the AlN formation is closely related to the formation of Nitrogen plasma during laser welding. In high power CO_2 laser welding the Nitrogen plasma is generated, while no plasma is formed in YAG laser welding. Therefore, the chemical reaction between Aluminium and Nitrogen is enhanced in CO_2 laser welding, while no reaction takes place in YAG laser welding.

As stated above, the use of a pure Nitrogen shield gas is somewhat useful to avoid the porosity and the increase in solute Nitrogen in austenitic stainless steel as well as the AlN formation in Aluminium alloys and this has been the general understanding in the world.
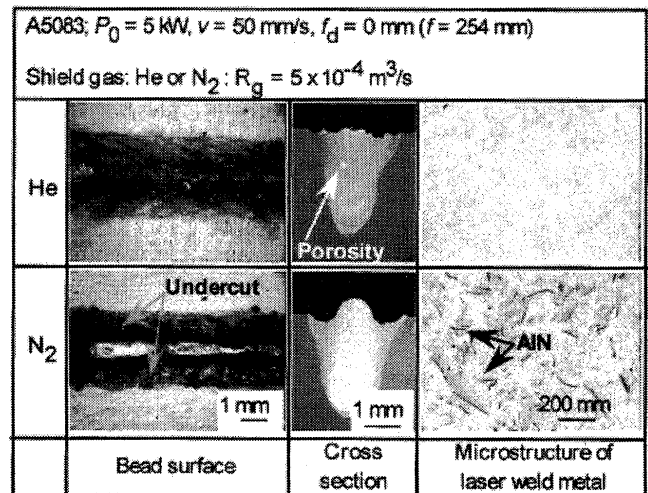
However, as seen in the previous Fig. 16, the Nitrogen shielding is also effective in reducing porosity in mild steel. This means that the above interpretation is not sufficient to explain the effect of Nitrogen shielding but there must be another reason.

The present authors have established that the characteristic large porosity in CW laser welding in an inert gas shield is associated by the instability of the keyhole[3-4]. However, the keyhole behaviour in a N_2 shield has not been observed. Hence, the authors conducted the simultaneous observation of keyhole dynamics and plasma behaviour in N_2 shielding condition and compared the difference of phenomena with those in a He shield.

Figure 21 shows pictures of laser induced plasma and X-ray images of keyholes in He shielding which are taken by two separate high speed video cameras. The figure is a composite of two pictures. In the He shielding, only metallic plasma is ejected from the keyhole opening and no He plasma is formed. The metallic plasma fluctuates its ejection direction and size. The keyhole is always formed during welding but its depth changes slightly and this fluctuation agrees well with the change of plasma behaviour. It was also observed that large metallic bubbles were formed, particularly at the keyhole bottom, and these bubbles mostly remained as the characteristic porosity.

Figure 22 shows the dynamic behaviour of the

Type 304 (8 mm^W); Bead on plate; P_0 = 15 kW, V = 25 mm/s, f_d = $\pm$0 mm (f = 381 mm),

Shielding gas: He, R_g = 8.5 x 10^{-4} m^3/s, n_f = 1,125 f/s.

t + 0 ms	t + 5.3 ms	t + 8.9 ms	t + 10.7 ms	t + 11.6 ms
t + 0 ms	t + 3.6 ms	t + 9.8 ms	t + 13.3 ms	t + 16 ms

Fig. 21 Dynamic behaviour of laser induced plasma and keyhole during CW CO$_2$ laser welding of stainless Steel in Helium shielding

Type 304 (8 mm^W); Bead on plate; P_0 =15 kW, v = 25 mm/s, f_d = $\pm$0 mm (f = 381 mm),

Shielding gas: N$_2$, R_g = 8.5 x 10^{-4} m^3/s, n_f = 1,125 f/s

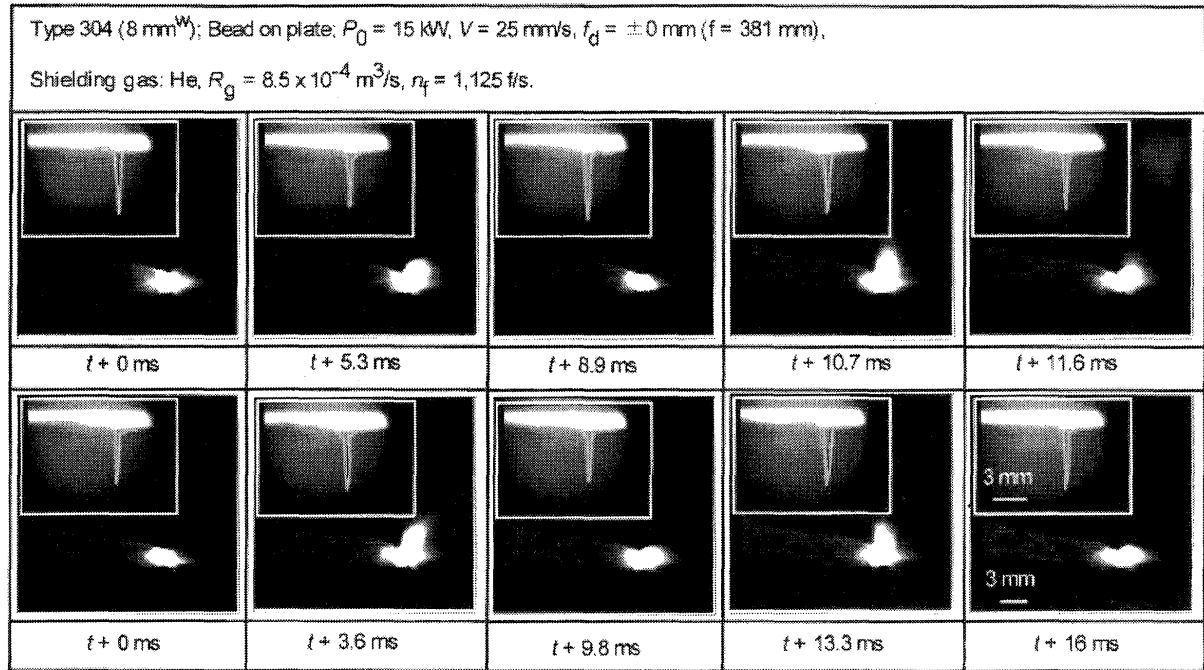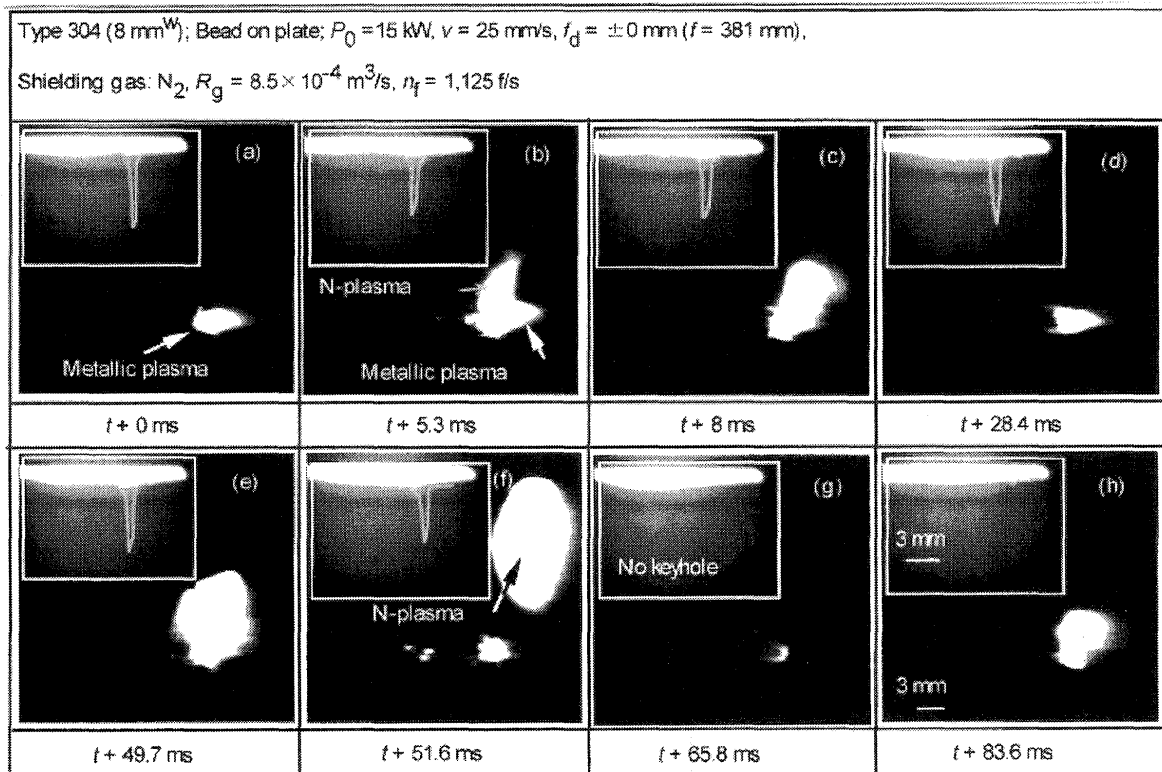| t + 0 ms	t + 5.3 ms	t + 8 ms	t + 28.4 ms
t + 49.7 ms	t + 51.6 ms	t + 65.8 ms	t + 83.6 ms

Fig. 22 Dynamic behaviour of laser induced plasma and keyhole during CW CO$_2$ laser welding of stainless Steel in Nitrogen shielding (Welding conditions are the same with Fig. 21)

laser induced plasma and keyhole during welding in N$_2$ shielding under the same welding condition as with Fig. 16. In the N$_2$ shield the phenomena are quite different from those in the He shield. Namely, two kinds of plasma, i.e., metallic and Nitrogen plasma, are formed intermittently as seen in the figure. Nitrogen plasma is

24

Table 2 Duration of metallic and Nitrogen plasma and equivalent pulse frequency and duty cycle in CO_2 laser welding in Nitrogen shield

Material	Duration (ms)	Metallic Plasma Duration (ms)	Nitrogen Plasma Duration (ms)	Frequency (Hz)	Duty Cycle (%)
A5083	24	13	11	40	52
Type 304	78	56	22	14	78
0.3%C Steel	337	298	39	3	91

ignited by the metallic plasma and it grows quickly upward and floats up from the weld pool. During the floating of N-plasma the metallic plasma disappears. When the N-plasma is extinguished, the metal plasma is again re-ignited. The depth of the keyhole becomes shallower during the growth of N-plasma and keyhole is completely closed when a large N-plasma ball is floating. The dynamic behaviour of the keyhole is very similar to that in modulated pulse welding in inert gas shielding in spite of CW welding. Moreover, it is characteristic that the metallic bubble formation in the keyhole is no longer observed in CW laser welding of Aluminium alloy and stainless steel with N_2 shielding. Namely, the self-excited pulsation takes place by the interaction between the incident beam and shield gas plasma. It is, therefore, concluded that the keyhole in N_2 shielded laser welding shuts down by itself before it becomes unstable and thus no porosity is formed as it was in the pulse modulation laser welding[4]. The authors also conducted the same experiments in Argon shield where Ar-plasma was always formed and no pulsation of keyhole took place. Therefore, the phenomena shown in Fig. 4 are the specific features when pure Nitrogen is used as the shield gas.

In **Table 2** are summarized the durations of metallic and Nitrogen plasma formation and equivalent pulse frequency and duty cycle in CW laser welding for three different base metals. As the self excited pulsation of N-plasma ignition and distinction is not uniform in periodicity, values in the table are statistically treated median values. It is noted that the duration of plasma formation, particularly metallic plasma duration as well as equivalent pulse parameters are strongly influenced by

the base metal. In mild steel the duration of metallic plasma is much longer than that in Al-alloy and stainless steel. Namely, duration of keyhole formation in mild steel is longer than in other materials. This mean that the keyhole instability is more likely to occur in mild steel compared with other materials. This is the reason that small amount of porosity remains in mild steel in the previous Fig. 18.

Conclusion

Major conclusions obtained in this work are as follows;

(1) The dynamic behaviours of the keyhole and laser induced plume in pulsed laser spot welding were observed simultaneously by the high speed videos and it was revealed that the keyhole fluctuated frequently in size and shape in spite of almost constant peak power during spot welding. Consistent with the keyhole fluctuation, the laser induced plume also appeared to generate and degenerate periodically and its periodicity was completely coincided with keyhole perturbation. The phenomenon took place in every metallic material used in this work but the fluctuation period was different depending on the material.

(2) When the pulsed laser power was quickly terminated, the keyhole opening collapsed within one tenth of the time that the whole weld pool solidified and a large cavity always formed at the bottom of keyhole.

(3) The keyhole as well as laser plume dynamics in CW laser welding were also observed by the optical and X-ray methods with high temporal resolution. The fluctuation of keyhole opening was less unstable than that in pulsed laser spot welding but still changed its shape and size with time. The periodic motion of the

keyhole opening well coincided with the cyclic tilting phenomenon of metallic plasma. The keyhole inside the molten pool, which was observed by X-ray transmission imaging system, revealed that the depth and shape of keyhole changed greatly with time. In particular a deep depression was formed on the rear wall of keyhole, which moved from the top to bottom periodically. A large bubble was seen when it came to the keyhole bottom and the bubble entered the molten pool, which resulted in the formation of characteristic porosity in laser welding. The gas analysis and SEM analysis of porosity showed that the bubble is composed of evaporated metal vapour and entrained shielding gas.

(4) The above results lead to a conclusion that the evaporation site in the keyhole was not uniform but changed its position with time, and the keyhole as well as whole molten pool was strongly perturbed by the dynamic pressure of metallic vapour jets. The liquid motion in the weld pool was also observed using small Tungsten particles preplaced between thin plates. It was revealed that there was a rapid complex flow in the molten pool, and metallic bubbles that contained the entrained shielding gas were moved by the swift flow and most of them could not float up to the surface but were trapped by the solidifying wall resulting in the porosity.

(5) The cavity formation caused by the keyhole fluctuation could be reduced or suppressed by stabilizing the keyhole. In pulsed laser spot welding, the addition of a proper tailing pulse was very effective in suppressing the porosity formation due to the gradual decrease of keyhole depth to avoid the sudden collapse of the keyhole opening. In CW laser welding, the controlled pulse modulation could effectively reduce the porosity formation by the forced oscillation of the keyhole. In this case, selection of optimum pulse frequency and duty cycle was essential.

(6) In the case of CW CO_2 laser welding, pure Nitrogen shielding is effective in suppressing the large porosity. It was found that the metallic plasma ignites the Nitrogen plasma intermittently and Nitrogen plasma grows large by the absorption of incident CO_2 laser beam and lifts off upward by the buoyancy force. During this period the incident beam is blocked by plasma and the keyhole disappears. When the Nitrogen plasma is extinguished at the upper part when the laser power density is low enough to sustain plasma, a new keyhole is again formed. Namely, the keyhole is repeatedly formed and extinguished in the same manner as in the pulse modulation welding. If the frequency and duty cycle of Nitrogen plasma formation and extinction are adequate, the keyhole instability is greatly reduced and porosity formation is effectively suppressed.

Acknowledgment

References

1) S. Katayama and others: "Pulse Optimization for Defect Prevention in Pulsed Laser Welding of Stainless Steel", Proc. of ICALEO'93, LIA (Laser Institute of America), Vol. 77, Oct. 24 – 28, 1993, Orlando, pp. 487 - 497.

2) A. Matsunawa: "Defects Formation Mechanisms in Laser Welding and Their Suppression Methods", Proc. of ICALEO'94, Vol. 79, Oct. 17-20, 1994,

Orlando, FL, USA, LIA, 203-209.

3) A. Matsunawa, J. D. Kim, S. Katayama and V. Semak: "Experimental and Theoretical Studies on Keyhole Dynamics in Laser Welding", Proc. of ICALEO'96, LIA, Vol. 81, Oct. 14-18, 1996, Detroit, pp. Section B58-67.

4) A. Matsunawa, J. D. Kim and S. Katayama: "Porosity Formation in Laser Welding – Mechanisms and Suppression Methods", Proc. of ICALEO'97, LIA, Vol. 83b, Part 2, Nov. 17-20, 1997, San Diego, pp. Section G73-82.

5) S. Katayama, M. Mizutani & A. Matsunawa: "Modelling of Melting and Solidification Behaviour during Laser Spot Welding", Science and Technology of Welding and Joining, Vol. 2 (1997), No. 1, pp.1 - 9.

6) A. Matsunawa, J. D. Kim, S. Katayama and T. Takemoto: "Spectroscopic Characteristics of Pulsed Laser-Induced Plume of Aluminum Alloys", The Review of Laser Engineering, Vol.. 24, No. 6 (1996), 679-688. (in Japanese)

7) Y. Arata: Plasma, Electron and Laser Beam Technology -Development and Use in Material Processing-, American Society for Metals (1986), 378 − 396.

8) P. G. Klemens: "Heat Balance and Flow Conditions for Electron Beam and Laser Welding", J. Appl. Phys., 47 (1976), 2165-2174.

9) T. Klein, M. Vicanek, J. Kroos, I. Decker and G. Simon: "Dynamic Behavior of the Keyhole in Laser Beam Welding", J. Phys. D: Appl. Phys., 27 (1994), 481-486.

10) J. Dowden, N. Postacioglu, M. Davis and P. Kapadia: "A Keyhole Model in Penetration Welding with A Laser", J. Phys. D: Appl. Phys. 20 (1987), 36-44.

11) D. Shuocker: "Modeling of Deep Penetration Welding with a Laser", Proc. of ICALEO'91, Orlando, FL., USA, Laser Institute of America (LIA), (1991), 32-39.

12) E. Metzbower: "Keyhole Formation", Metall. Trans. B, 24 (1993), 875-880.

13) J. Kroos, U. Gratzke and G. Simon: "Towards a Self-Consistent Model of the Keyhole in Penetration Laser Beam Welding", J. Phys. D: Appl. Phys., 26

(1993), 481-486.

14) A. Kaplan: "A Model of Deep Penetration Laser Welding Based on Calculation of the Keyhole Profile", J. Phys. D: Appl. Phys., 27 (1994), 1805-1814.

15) J. Dowden, and P. Kapadia: "A Mathematical Investigation of the Penetration Depth in Keyhole Welding with Continuous CO_2 Laser", J. Phys. D: Appl. Phys., 28 (1995), 2252-2261.

16) N. Postacioglu, P. Kapadia and J. Dowden: "Theory of the Oscillations of an Ellipsoidal Weld Pool in Laser Welding", J. Phys. D: Appl. Phys., 24 (1991), 1288-1292.

17) T. Klein, M. Vicanek, J. Kroos, I. Decker and G. Simon: "Oscillations of the Keyhole in Penetration Laser Beam Welding", J. Phys. D: Appl. Phys., 27 (1994), 2023-2030.

18) V. V. Semak, J. A. Hopkins, M. H. McCay and T. D. McCay: "Dynamics of Penetration Depth during Laser Welding", Proc. ICALEO'94, Orlando, FL., USA, LIA, (1994), 830-837.

19) V. V. Semak, J. A. Hopkins, M. H. McCay and T. D. McCay: "Melt Pool Dynamics during Laser Welding", J. Phys. D: Appl. Phys., 28 (1995), 2443-2450.

20) R. Fabbro and A. Poueyo-Verwaerde: "Modeling of Deep Penetration Laser Welding Process – Application to the Analysis of the Energy Coupling inside the Keyhole-", Proc. Of ICALEO'95, Orlando, FL., USA, LIA (1995), 979-988.

21) A. Matsunawa and V. Semak: "The Simulation of Front Keyhole Wall Dynamics during Laser Welding", J. Phys. D: Appl. Phys., 30 (1997), 798-809.

22) V. Semak and A. Matsunawa: "Role of The Recoil Pressure in Energy Balance during Laser Welding", J. Phys. D: Appl. Phys. 30 (1997), 2541-2552.

23) S. Satoh and others: "Influence of Shielding Gas and Laser Irradiation Conditions on Porosity Formation in CO_2-Laser Welding of Aluminum Alloy", J. of Light Metal Welding and Construction, Vol. 35, No. 9 (1997), 409 - 416. (in Japanese)

24) A. Otto and others: "Nonlinear Dynamics during Laser Beam Welding", Proc. of ICALEO'96, LIA, Vol. 81, Oct.14-17, 1996, Detroit, Sec. B. 30-39.